Atmospheric Environment 99 (2014) 556–567

Contents lists available at ScienceDirect

Atmospheric Environment

journal homepage: www.elsevier.com/locate/atmosenv

Airborne measurements of HC(O)OH in the European Arctic: A winter – summer comparison

Benjamin T. Jones [a], Jennifer B.A. Muller [a], Sebastian J. O'Shea [a], Asan Bacak [a], Michael Le Breton [a], Thomas J. Bannan [a], Kimberley E. Leather [a], A. Murray Booth [a], Sam Illingworth [a], Keith Bower [a], Martin W. Gallagher [a], Grant Allen [a], Dudley E. Shallcross [b], Stephane J.-B. Bauguitte [c], John A. Pyle [d], Carl J. Percival [a, *]

[a] *Centre for Atmospheric Science, School of Earth, Atmospheric and Environmental Science, University of Manchester, Oxford Road, Manchester M13 9PL, UK*
[b] *School of Chemistry, University of Bristol, Cantock's Close, Bristol BS8 1TS, UK*
[c] *Facility for Airborne Atmospheric Measurements (FAAM), Building 125, Cranfield University, Cranfield, Bedford MK43 0AL, UK*
[d] *National Centre for Atmospheric Science – Climate, Department of Chemistry, University of Cambridge, Cambridge CB2 1EW, UK*

HIGHLIGHTS

- The first airborne measurements of HC(O)OH in the European Arctic (EA).
- No significant HC(O)OH snowpack source was observed during winter measurements.
- Averaged HC(O)OH concentrations suggest marine sources dominate over land sources.
- Calculations suggest CH_2I_2 oxidation represents a major marine source in the EA.

ARTICLE INFO

Article history:
Received 9 July 2014
Received in revised form
14 October 2014
Accepted 15 October 2014
Available online 16 October 2014

Keywords:
Organic acids
Formic acid
Criegee intermediate
Diiodomethane
Arctic
CIMS

ABSTRACT

This study represents the first airborne, in-situ measurements of HC(O)OH in the European Arctic, across the winter and summer seasons. HC(O)OH concentrations are under predicted at present, particularly in the mid to high northern latitudes. Data presented here probe unconfirmed sources of HC(O)OH in the Arctic, and would suggest an ocean source of HC(O)OH is more significant than proposed land sources in both winter and summer environments. A maximum concentration of 420 ppt was recorded over the ocean during the July 2012 campaign. This was more than 1.7 times greater than the maximum land concentration reported. Calculated estimates on HC(O)OH production would suggest diiodomethane photolysis could represent a significant source of HC(O)OH in marine environments in the European Arctic. Enhanced HC(O)OH concentrations observed at altitudes greater than 2 km particularly during the March campaign highlight the significance of long range transport on the European Arctic budget. In addition, two HC(O)OH vertical profiles between the altitudes 0.3–6.6 km are presented to provide a more representative vertical profile for this latitude which may be used to improve forthcoming regional and global modelling of the HC(O)OH budget.

1. Introduction

Carboxylic acids are important, ubiquitous compounds found in the troposphere and have been detected in both the gas and aerosol phase (Paulot et al., 2011; Le Breton et al., 2011, 2013a). HC(O)OH (formic acid) and $CH_3C(O)OH$ (acetic acid) are considered to be the most abundant of these acids and have a low reactivity to gas phase reactions with the oxidants; OH and NO_3 radicals and O_3 (Chebbi and Carlier, 1996). These acids can contribute significantly to tropospheric free acidity, and represent up to 90% of the total rainwater acidity in remote, non-urban environments (Andreae et al., 1988). HC(O)OH emission from tundra soil and wetlands are expected in the Arctic, although no direct measurement has been documented in the region. Assuming a soil temperature of 303 K, Paulot et al. (2011) inferred tundra soil and wetland emissions of 1.44 nmol m^{-2} min^{-1} and 0.9 nmol m^{-2} min^{-1} respectively, based on modelled NO (nitrogen monoxide) emissions over tundra soil and wetland environments (Yienger and Levy, 1995). Previous

* Corresponding author.
E-mail address: c.percival@manchester.ac.uk (C.J. Percival).

http://dx.doi.org/10.1016/j.atmosenv.2014.10.030
1352-2310/© 2014 Published by Elsevier Ltd.

studies have reported that HC(O)OH soil emission exhibits a strong temperature dependence (Sanhueza and Andreae, 1991), therefore soil emissions within the Arctic region are likely to be significantly reduced. HC(O)OH is also emitted from several tree species, most notably from the Norwegian Spruce, a common constituent in northern Scandinavia (Kesselmeier et al., 1998). Kesselmeier et al. (1998) reported summer emission rates (±one standard deviation) of 0.83 (±0.14) nmol m^{-2} min^{-1} and 0.49 (±0.08) nmol m^{-2} min^{-1} for the Norwegian Spruce in light and dark environments respectively, indicative of a diurnal pattern. These emission rates were measured at constant temperatures of 300 K in the light and 295 K in the dark, which highlight the influence of temperature. The lower temperatures expected in the high latitudes are likely to reduce or possibly inhibit tree emissions of this type. An ocean emission source may also contribute to the Arctic HC(O)OH budget (Graedel and Weschler, 1981). Indeed, Baboukas et al. (2000) observed a mean HC(O)OH concentration of 360 ppt at the latitude 63°N aboard a research vessel over the North Atlantic Ocean in October 1996. Furthermore, Legrand et al. (2004) attributed concentrations of up to 200 ppt observed at a coastal site in Antarctica to the transport of oxidised organics released by phytoplankton in the ocean. The relatively high HC(O)OH concentrations collected over the ocean would suggest this marine source of HC(O)OH may contribute significantly to the Arctic budget, however a lack of understanding of the mechanism and the limited datasets over marine environments, particularly in the high latitudes, complicates the significance of such sources to the Arctic atmosphere. HC(O)OH's dominant removal pathways are considered to be wet and dry deposition, rather than gas-phase reactions (Baboukas et al., 2000). Therefore HC(O)OH is considered to favourably partition from the gaseous phase into the liquid phase in the presence of water, which would further complicate the interpretation of sources within marine environments. Further to these direct emission sources, secondary production predominantly from alkene ozonolysis of biogenic precursors, is thought to be a major source of HC(O)OH (Jacob and Wofsy, 1988; Leather et al., 2011). A more novel source of HC(O)OH may arise from the photolysis of diiodomethane (CH_2I_2) in the atmosphere which will lead to a small but non negligible source of the criegee intermediate (CH_2OO), which can then react with water vapour to yield HC(O)OH (Shallcross, personal communication; Welz et al., 2012). Other known sources of HC(O)OH that are likely to effect the Arctic budget include vehicle emission (Kawamura et al., 1985; Talbot et al., 1988; Le Breton et al., 2011; Bannan et al., 2013) predominantly from urban environments, and biomass burning (Talbot et al., 1990), commonly from boreal forests. HC(O)OH's lifetime in the free troposphere is estimated to be 3.2 days due to its relatively slow reactivity with the hydroxyl radical (OH) in the atmosphere (Paulot et al., 2011). Therefore, long range transport of these sources may play a significant role in the Arctic atmosphere. Despite our understanding of a number of HC(O)OH sources and sinks, their relative contributions to the Arctic budget remain highly uncertain, particularly in the European Arctic where HC(O)OH concentrations have scarcely been documented.

1.1. Arctic HC(O)OH measurements

Current Global Chemistry Transport Model predictions suggest sources in the high latitudes do not significantly contribute to the global HC(O)OH budget (Stavrakou et al., 2011), most likely due to lower anthropogenic influence and the cold Arctic temperature reducing biogenic activity. However, current models have been found to substantially under-predict HC(O)OH levels in the northern mid to high latitudes (Stavrakou et al., 2011; Gonzalez Abad et al., 2009). Measurements by the IASI satellite in the high latitudes report concentrations up to five times greater than model predictions, which cannot be accounted for by current source inventories (Stavrakou et al., 2011). The application of thermal contrast filters to reduce the total column error for the IASI retrievals limits satellite measurements over the high altitudes and excludes data collected over the ocean (George et al., 2009). This is an inherent limitation in satellite measurements and highlights the need for additional in-situ data to supplement satellite data and prevent the transfer of biases into global transport models. Several HC(O)OH measurements collected over high latitudes show a distinct bias towards the growing season which would seemingly highlight the influence of biogenic sources (Gonzalez Abad et al., 2009: Grutter et al., 2010). Indeed, Grutter et al. (2010) reported satellite HC(O)OH concentrations at an altitude of 10 km of up to 90 ppt in July 2007, where concentrations fell in December 2007 to 27 ppt highlighting this seasonal change in the Arctic. Gonzalez Abad et al. (2009) reported several HC(O)OH concentration hot spots associated with biomass burning events over the high latitudes with concentrations reaching up to 590 ppt at an altitude of 6.5 km. Long range transport of these large biomass burning events is expected to influence the Arctic, but their contribution to the HC(O)OH budget remains unclear.

Currently, there are very few in-situ measurements of HC(O)OH within the Arctic Circle. Talbot et al. (1992) reported a summer mean concentration of 270 ppt between the altitudes 0.15–2 km over the North American Arctic. Measurements collected at Summit, Greenland in 1993 showed a summer mean concentration of 1198 ppt (Dibb et al., 1994), with mean summer values of 650 ppt and 750 ppt for the following years 1994 and 1995, far exceeding modelled predictions (Dibb et al., 1998). The large variability between data-sets highlights the need for further measurements in this region. Furthermore, these elevated levels have led to the suggestion of possible missing sources in the high latitudes. Dibb and Arsenault (2002) suggested that a snowpack emission source of HC(O)OH via oxidation of organic compounds on snow grains within the interstitial air may contribute. Measurements of up to 300 ppt were reported within the interstitial air of the Alaskan snowpack, which decreased by a factor of three at the same location 6 m above the snow (Gao et al., 2012). The impact of this snow source on the Arctic HC(O)OH budget in the European Arctic has yet to be evaluated.

To our knowledge, no airborne measurements have been documented in the European Arctic. This study presents the first airborne measurements of HC(O)OH in the European Arctic to investigate the influence of seasonality on local and long range source emissions in the European Arctic. Furthermore, these measurements serve to investigate the contributions of known and potentially unknown source emissions to the regional HC(O)OH budget and to hypothesise reasons for the differences between modelled and measured data in the high latitudes. In addition, vertical profiles of HC(O)OH are highly uncertain, with very few documented a priori profiles in the high latitudes (Razavi et al., 2011). Therefore this work includes summer vertical profiles to provide a more representative vertical profile of HC(O)OH in the European Arctic for use in satellite validation retrieval.

2. Experimental

A Chemical Ionisation Mass Spectrometer (CIMS) was used for in-situ measurement of HC(O)OH on board the FAAM BAe-146 aircraft at a 1 Hz frequency. The CIMS instrument was constructed by Georgia Institute of Technology as described by Nowak et al. (2007), and set up on the FAAM BAe-146 aircraft as illustrated by Fig. 1 (Le Breton et al., 2011, 2013b; 2013b).

Sample air (12 SLM) is drawn through a heated inlet (313 K) by a rotatory vane pump (Picolino VTE-3, Gardner Denver Thomas) at

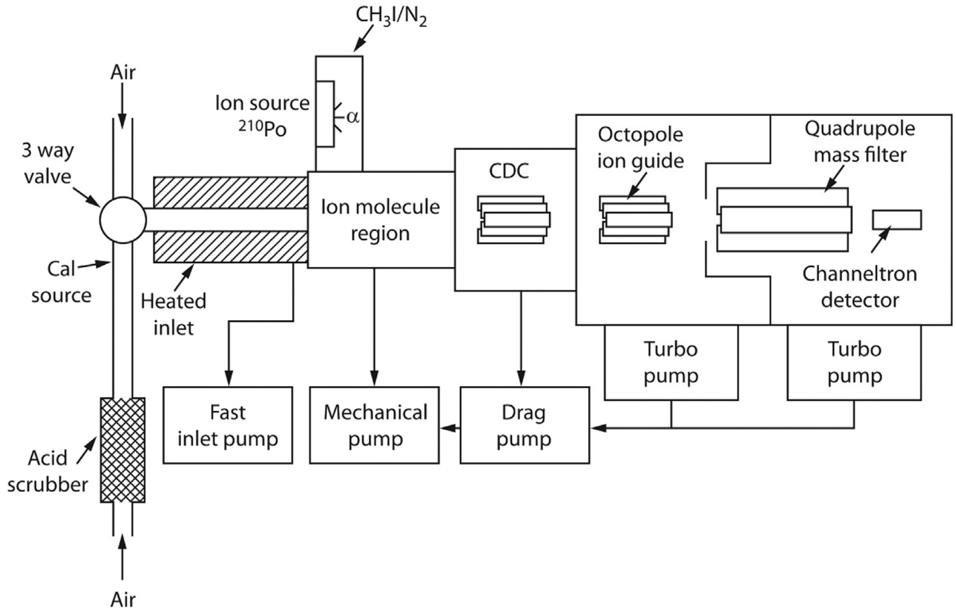

Fig. 1. Schematic of Manchester CIMS.

atmospheric pressure, controlled by a limiting orifice. Air is sub-sampled by a pinhole (380 µm) at a flow rate of 0.8 SLM into the ion molecule region, where the acid species are ionised, held at a constant pressure (20 Torr) by a mechanical scroll pump. The ionised species are subsequently drawn through an aperture held at a potential to focus the charged species into a collision dissociation chamber (CDC).

The collision dissociation chamber is pumped by a molecular drag pump (MDP-5011, Adixen Alcatel Vacuum Technology), backed by a mechanical scroll pump and held at approximately 1 Torr. The CDC serves to dissociate weakly bound cluster ions via energetic collisions and produce core-ions ready for detection. The ions are moved to an octopole ion guide held at a pressure of 10^{-3} Torr by a turbomolecular pump (V-81 M Navigator, Varian Inc. Vacuum Technologies), where the ions collimate. Ions are then focused into a quadrupole mass filter with pre and post filters by entrance and exit lenses (Tri-filter Quadrupole Mass Filter, Extrel CMS). The quadrupole mass filter uses the stability of the trajectories in the oscillating electric fields to separate and filter the ions according to their mass to charge ratio (m/z). The selected ions are then detected and counted by a continuous dynode electron multiplier (7550 M detector, ITT Power Solutions, Inc.) at a pressure of 10^{-6} Torr using a second turbomolecular drag pump (V-81 M Navigator, Varian Inc. Vacuum Technologies).

2.1. The ionisation scheme

The soft ionisation technique used for trace gas detection in this system utilised an iodide ion scheme previously described by Slusher et al. (2004) for the detection of HC(O)OH (Le Breton et al., 2011). A CH_3I (methyl iodide) and H_2O gas mixture in N_2 was added (1 SCCM) to a flow of N_2 (2 SLM), and passed over a radioactive ^{210}Po source. The ^{210}Po source is an α-emitter and initiates a dissociative electron attachment reaction with methyl iodide to form the reagent ion (R1). The reagent ion is passed into the ion molecule region where it combines with HC(O)OH species via an adduct reaction (R2). This enables detection of HC(O)OH at $m/z = 173$ (I^-.[HC(O)OH]).

$$2CH_3I/H_2O/N_2 + He^{2+} \rightarrow 2I^- \cdot (H_2O)_n \qquad \text{R1}$$

$$I^- \cdot (H_2O)_n + HC(O)OH \rightarrow I^- \cdot [HC(O)OH] \cdot (H_2O)_n \qquad \text{R2}$$

2.2. Instrumental background and sampling method

The CIMS inlet is split into background-calibration and sample inlets, controlled by a 3-way solenoid valve to regulate the inlet air pathway. In the sample inlet, ambient air is drawn through a heated inlet (313 K), passing through the controlled 3-way solenoid valve and air is entered directly into the CIMS. In the background-calibration inlet, air is drawn through an alternative heated inlet (313 K) and through a scrubber system before entering the CIMS. The scrubber system used in this study consisted of a single coil of nylon filings coated and dried with sodium carbonate to establish an instrumental background. Instrumental backgrounds were collected at selected times during each flight and were removed from the final data. HC(O)OH calibrations were performed on each flight using a 0.005% HC(O)OH gas mixture. A flow (10 SCCM) of HC(O)OH was introduced into the CIMS at a stable altitude/ground level with scrubbed ambient air, with the change in HC(O)OH signal corresponding to the concentration of the cylinder. Calibrations were conducted on each flight and the sensitivity was calculated and applied to each data set. The calibration HC(O)OH gas mixture (of 0.005%) was prepared using a high pressure manifold, where liquid HC(O)OH was expanded into a cylinder (23 Torr), and subsequently diluted in N_2 gas pressurised up to 2280 Torr. This gas mixture was then diluted further by removal of gas mixture to a pressure of 11.4 Torr, and subsequently pressurised up to 2280 Torr resulting in a 0.005% HC(O)OH gas mixture. The final concentration of the calibration cylinder was then validated after the campaign using GC-FID analysis. The CIMS inlet line and calibration method has been further described in Le Breton et al. (2011).

2.3. Ionisation efficiency calibration

Slusher et al. (2004) identified a water vapour dependence on the efficiency of ionising organic acids using an iodide anion reagent within a CIMS instrument. In order to account for this dependency, water vapour was added to the ionisation gas mixture to produce a surplus of $I^- \cdot H_2O$ cluster ions and thereby limit the effect of water on instrument sensitivity. For this instrument set up however, a linear decrease in sensitivity remained for HC(O)OH within lower relative humidity conditions. A $I^- \cdot H_2O$ sensitivity is also apparent for instrument background values of HC(O)OH. In order to account for this second effect, a water specific background HC(O)OH concentration is calculated before each measurement period (prior to each flight). Instrument background signal counts of mass 173 representing $I^- \cdot$HC(O)OH, were monitored in relation to changing $I^- \cdot H_2O$ counts observed at mass 145. $I^- \cdot H_2O$ counts were controlled by altering set flows of dry N_2 (ranging between 0 and 10 SLM dry N_2) entering the sample inlet of the CIMS instrument. The dry nitrogen was combined with scrubbed ambient air diluting the $I^- \cdot H_2O$ ions entering the CIMS instrument. The scrubbed air is produced by passing ambient air through a scrubber containing sodium carbonate coated nylon filings which act as a method of removing air contaminants within the air flow entering the CIMS (Le Breton et al., 2011). Fig. 2A illustrates the change in $I^- \cdot$HC(O)OH background counts as the $I^- \cdot H_2O$ counts are adjusted. This plot is then used to provide a calculated instrument background for $I^- \cdot$HC(O)OH counts across the range of $I^- \cdot H_2O$ counts, which is then subtracted from the measured data to obtained corrected $I^- \cdot$HC(O)OH counts. Furthermore, a second calibration is required to correct the $I^- \cdot H_2O$ dependency on HC(O)OH enhancements as well. This is done by adding a known concentration of HC(O)OH to scrubbed ambient air, where the change in $I^- \cdot$HC(O)OH counts from its background counts is used to calculate a sensitivity. Subsequently the calibration sample flow is then diluted by set flows of dry N_2 where the sensitivity change is monitored in relation to the change in $I^- \cdot H_2O$ counts. This calibration shows a linear relationship between $I^- \cdot H_2O$ counts and HC(O)OH sensitivity as illustrated by Fig. 2B. Ultimately a corrected instrument background for $I^- \cdot$HC(O)OH counts is removed from the measured data and a water-specific sensitivity for HC(O)OH enhancements is also applied to the data. Water specific background calibrations were performed daily, prior to each flight and the corrected instrument background was removed from each flight data. Water-specific HC(O)OH sensitivity calibrations were also performed daily during the measurement period and applied to the data for each flight.

3. Campaign outline

3.1. MEVALI

Two short campaigns were completed over the European Arctic during the winter and summer seasons. The first campaign was conducted on the 10–18th March 2012, as part of a UK Met. Office project, Microwave Emission Validation over sub-Arctic Lake Ice (MEVALI). The primary focus of this campaign was to validate a Met. Office microwave emissivity model from snowpack backscatter in the Arctic. A subsequent part of the project was to investigate these layered snow packs as a potential source of HC(O)OH. This campaign consisted of 6 flights with a total of 460.5 airborne data minutes. During the winter campaign, low level stratus and stratocumulus clouds were observed on occasion. No precipitation events were observed during the flights, although light snowfall had occurred on some of the nights prior to measurements. The mean surface temperature for the base station in Kiruna during the March campaign was 269 K. The 3σ limit of detection for HC(O)OH during the winter campaign was 20 ppt and the average in-flight calibration sensitivity for HC(O)OH was 34.2 (±0.5) ion counts s^{-1} ppt^{-1}. The flight tracks taken during the MEVALI campaign are illustrated by Fig. 3, where the date and duration of each flight are detailed in Table 1. In total, 279 min of data were collected over land, and 181.5 min of data were obtained over a marine environment during the campaign.

3.2. MAMM

A short second campaign was completed between the 20–23rd July 2012 as part of a NERC (UK Natural Environment Research Council) funded project named; Methane and other greenhouse gases in the Arctic, Measurements, process studies and Modelling, abbreviated to MAMM. The primary objectives for this study were to investigate sources of methane and other trace gases, as well as validating satellite (IASI/SCIAMACHY) column measurements with in-situ data in the Arctic. This campaign consisted of four flights of measurement data and represented a total of 406.5 min of aircraft data. Low level stratocumulus clouds were also observed for the summer campaign and the mean surface temperature for the base station in Kiruna was 282 K. Snow cover was only observed on mountain tops at high altitudes over Svalbard. The 3σ limit of detection for HC(O)OH during the summer campaign was 24 ppt and the average in-flight calibration sensitivity for HC(O)OH was 11.6 (±0.3) ion counts s^{-1} ppt^{-1}. Instrument HC(O)OH sensitivity is dependent on the observed $I^- \cdot H_2O$ species detected. The factors which affect the number of $I^-.H_2O$ species include relative humidity, water content within the ionisation gas cylinder (CH_3I) and the ^{210}Po emission variability, as a result of its six month half-life. These variations however are taken into account by daily, water-specific background calibrations, as well as daily HC(O)OH

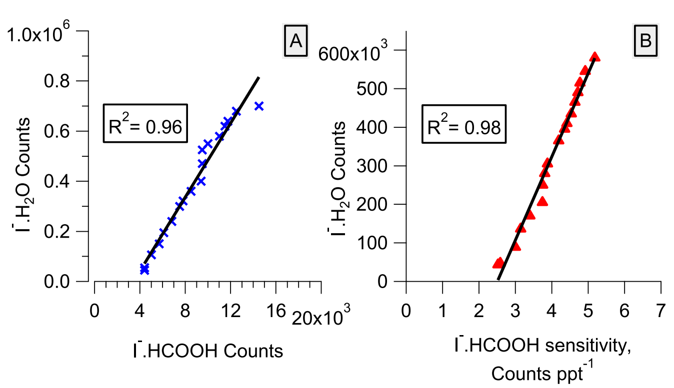

Fig. 2. A(left): A graph to show the linear relationship observed between changing m/z 145 (representing H_2O content) and background (m/z 173 representing HC(O)OH). B(right): represents the linear relationship between HC(O)OH sensitivity and H_2O content (representing m/z 145) during an HC(O)OH calibration.

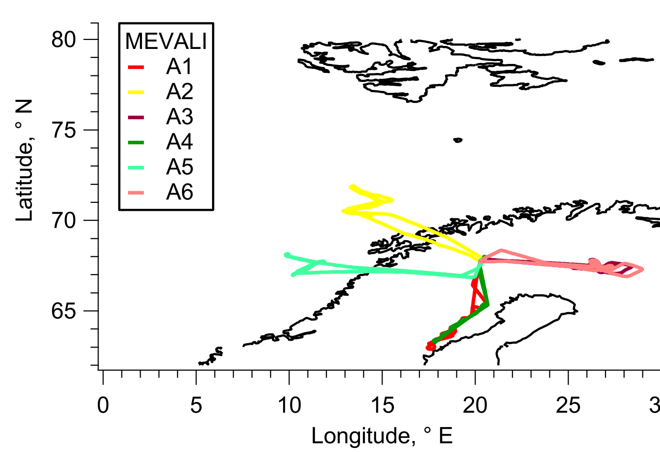

Fig. 3. An outline of the flight tracks (A1-A6) for campaign A (MEVALI) during March 2012.

Table 1
Outlines the flight date and time for each flight during the MEVALI campaign based out of Kiruna, Sweden.

Fig. 3: Legend (flight reference)	Flight date	Local time of flight, utc
A1 (B679)	10th March 2012	07:00:00–12:10:00
A2 (B681)	13th March 2012	10:57:00–16:01:00
A3 (B682)	14th March 2012	07:49:30–12:38:00
A4 (B863)	14th March 2012	15:03:00–20:19:00
A5 (B684)	16th March 2012	09:41:30–14:58:00
A6 (B685)	18th March 2012	08:51:00–13:59:00

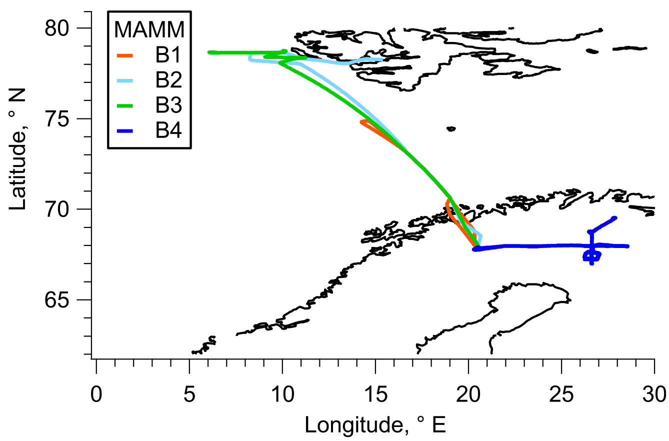

Fig. 4. An outline of the flight tracks (B1 – B4) for the July (MAMM) campaign.

sensitivity calibrations across a range of stable $I^- \cdot H_2O$ counts. Furthermore, this sensitivity effect illustrates the importance of the $I^- \cdot H_2O$ calibration technique for measuring HC(O)OH for this specified CIMS set up. The flight tracks taken during the MAMM campaign are illustrated by Fig. 4, where the date and duration of each flight are detailed in Table 2. In total, 147 min of data were collected over land, and 259.5 min of data were obtained over marine environments during the campaign.

Potential temperature data collected during vertical profiles during each campaign were used to estimate boundary layer heights (BLH)'s for each flight. BLH's were highly variable in both the summer and winter campaigns, reaching a maximum observed BLH of 1.2 km in winter, and 1.5 km in summer. In order to provide a qualitative comparison between these seasons, HC(O)OH data within an altitude limit of 1.5 km were selected to provide more insight into local source emissions and the seasonality influence on these local sources within the European Arctic.

4. Results and discussion

4.1. Flight campaign comparisons

HC(O)OH measurements for each campaign were collected across the same altitude range of 0.3–7 km. Data acquisition from

Table 2
Outlines the flight date and time for each flight during the MAMM campaign based out of Kiruna, Sweden.

Fig. 4: Legend (flight reference)	Flight date	Local time of flight, utc
B1 (B717)	20th July 2012	13:52:30–17:23:00
B2 (B718)	21st July 2012	09:28:30–13:17:00
B3 (B719)	21st July 2012	15:19:00–18:35:00
B4 (B720)	22nd July 2012	10:55:00–16:09:00

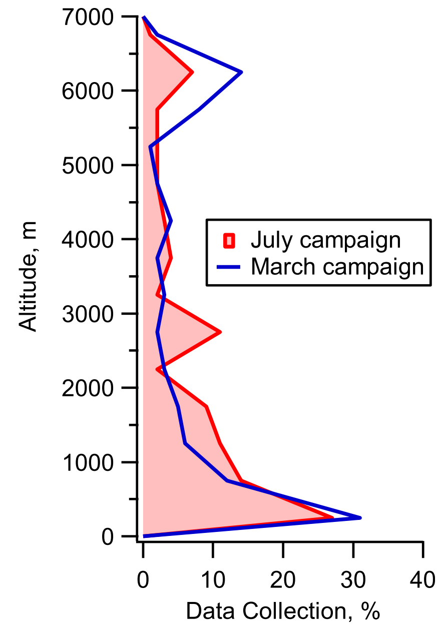

Fig. 5. Identifies the percentage data acquired between the two campaigns (MEVALI and MAMM) in relation to 500 m altitude bins across an altitude range of 0.5–7 km.

each campaign was obtained over comparable altitude bins, as shown in Fig. 5. Box and whisker plots are also illustrated by Fig. 6 to assess the variability between flights for each campaign.

4.1.1. MEVALI (March) flight variability

As illustrated by Fig. 6, concentrations between flights were consistently low with the exceptions of flight A2 and flight A5. HC(O)OH vertical profiles for flights A2 and A5, as shown by Fig. 7A and B, identified elevated concentrations at altitudes $\leq$1.5 km. Interestingly, these two flights were conducted predominantly over the ocean unlike the remaining flights, which may suggest an ocean source may be responsible. With regards to flight A2, an HC(O)OH peak of 424 ppt was observed during a decent at altitude 1.4 km over the ocean where the concentration gradually decreased to 325 ppt at altitude 0.3 km. No comparable trend was observed in

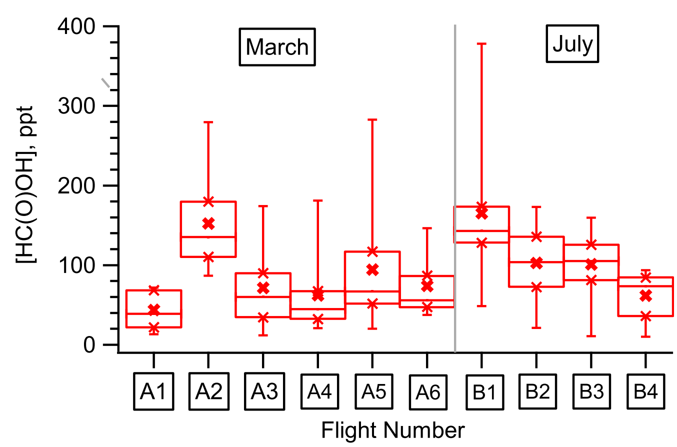

Fig. 6. HC(O)OH Box plots of the winter (March) and summer (July) campaigns collected over the European Arctic in ppt, where the x signifies the mean concentration, and the box and whisker plots are divided into 5 and 95% percentiles, 25% and 75% percentiles represented by the box, the median represented by the central line within the box and the mean is represented by the x. The flight numbers are in reference to those described in Tables 1 and 2.

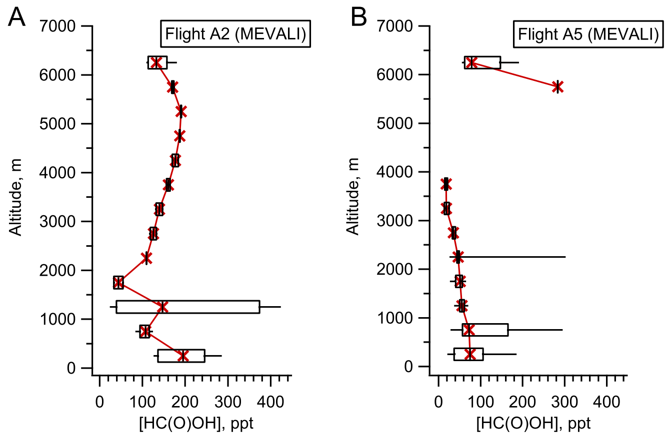

Fig. 7. A(left): represents the HC(O)OH vertical profile of measurements taken on flight A2 on the 13th March 2012. B(right): represents the HC(O)OH vertical profile of measurements taken on flight A5 on the 16th March 2012. The profiles have been split into data bins of 0.5 km altitude. The box and whisker plots are divided into 10 and 90% percentiles, 25% and 75% percentiles represented by the box, the median represented by the central line within the box and the mean is represented by the *x* highlighted in red. (For interpretation of the references to colour in this figure legend, the reader is referred to the web version of this article.)

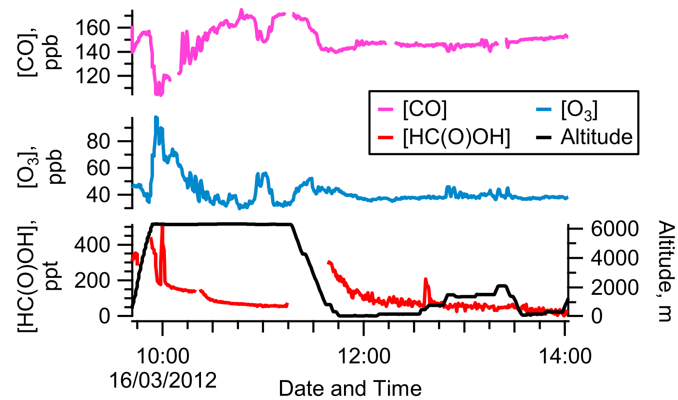

Fig. 9. Illustrating the concentration change in HC(O)OH during flight A5 with respect to altitude and the trace gas species; O_3 and CO concentrations. The data gaps at 9:57–10:00 utc and 11:37–11:50 represent background sampling points.

CO and O_3 tracer species at this point, as shown by Fig. 8, signifying anthropogenic influence was minimal. Furthermore, a relatively low O_3 concentration ranging between 31 and 35 ppb, showed no correlation with HC(O)OH, indicating secondary production via ozonolysis was also not a significant contributor at this point in the flight. Four day HYSPLIT backward trajectory analysis of the increased concentration of HC(O)OH at altitude 1.4 km revealed the air mass had remained within the Arctic circle, and predominantly at altitudes $\leq$1 km over the ocean surface, suggesting the rise may be the result of a local marine source. In addition, Fig. 7A also illustrates a steady HC(O)OH increase above the altitude bin of 1.5 km–5.5 km from 39 ppt to 180 ppt for flight A2. This would indicate long range sources may also be influencing HC(O)OH at high altitudes.

With regards to flight A5, two HC(O)OH enhancements were observed showing a rise of 142 ppt and 341 ppt at times 09:53:30 and 10:00:00 UTC respectively, as shown by Fig. 9. The first elevation of HC(O)OH showed a clear positive gradient with CO 4.29 ($\pm$0.86) ppt ppb^{-1} with an R^2 of 0.81. Contrastingly, this HC(O)OH peak was found to strongly anti-correlate with O_3 with a gradient of $-$3.62 ($\pm$0.71) ppt ppb^{-1} and an R^2 of 0.81. This information would suggest the HC(O)OH peak was likely the result of a direct emission source, however the relatively high O_3 levels from 50 ppb to 80 ppb and high altitude during the period of enhancement further complicate the source assignment or exclusion. Contrastingly, the second elevation of HC(O)OH revealed no significant correlation with CO or O_3, at much lower CO levels (120 ppb) and much higher O_3 concentrations (68 ppb). As a result the source origin of these increased levels of HC(O)OH could not be assigned. Four day HYSPLIT backward trajectories identified the air masses travelled from a west direction and remained at high altitudes. The trajectories would suggest the lowest distances travelled in altitude by the air masses were 3.5 km and 2.8 km respectively, and descended at the same location situated south west of the Icelandic coast. Although it would appear that long range sources from outside of the European Arctic may influence HC(O)OH concentrations in the region at high altitudes, identification of long range

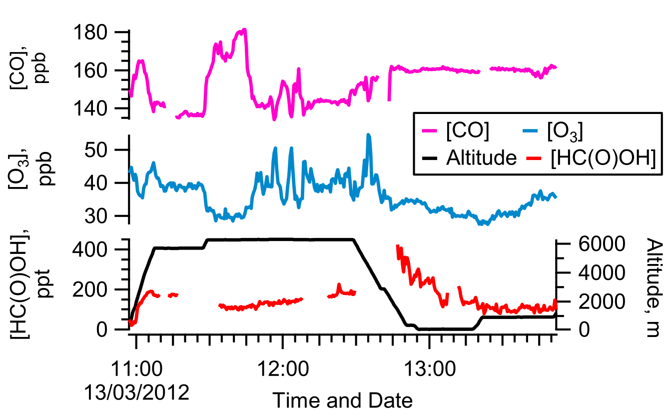

Fig. 8. Illustrating the concentration change in HC(O)OH during flight A2 with respect to altitude and the trace gas species; O_3 and CO concentrations. 11:20–11:35 UTC represents a calibration and the remaining data gaps represent periods of background sampling.

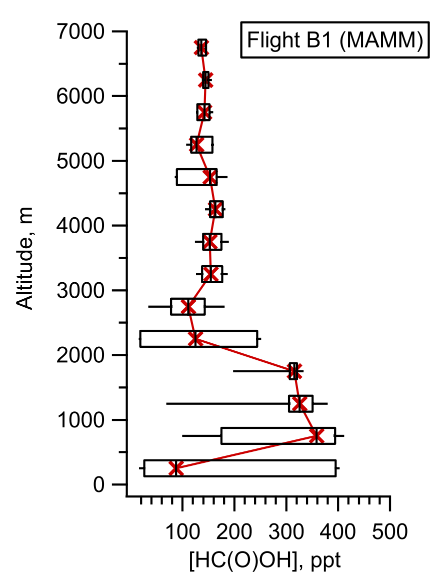

Fig. 10. Represents the HC(O)OH vertical profile of measurements taken on flight B1 on the 20th July 2012, where the profile has been split into data bins of 500 m altitude. The box and whisker plots are divided into 10 and 90% percentiles, 25% and 75% percentiles represented by the box, the median represented by the central line within the box and the mean is represented by the x highlighted in red. (For interpretation of the references to colour in this figure legend, the reader is referred to the web version of this article.)

sources from these events is beyond the scope of this paper. The influence of local HC(O)OH sources however will be discussed further in sections 4.2–4.5.

4.1.2. MAMM (July) flight variability

In regards to the MAMM summer campaign, Fig. 6 identifies flight B1 to have a higher mean concentration for HC(O)OH and is significantly more variable in comparison to the rest of the flight campaign. The data collected during this flight were predominantly collected over the ocean and the highest HC(O)OH concentrations were observed in the lowest altitude bin, as shown in Fig. 10. This enhancement was observed over the ocean between 16:18 and 16:24 UTC. As shown in Fig. 11, O_3 and CO levels remained at low background levels of 24 ppb and 90 ppb respectively, indicating anthropogenic emissions are low and unlikely to contribute to the observed rise in HC(O)OH. Four day HYSPLIT backward trajectory analysis of the HC(O)OH peak over the ocean, identified the air mass to be from a northern origin and remained close in proximity ($\leq$0.5 km) to the ocean's surface, not passing over any land surface. This would indicate the source of this HC(O)OH elevation was likely to be local and of a marine origin. Flights B2 and B3 were also conducted over the ocean (in the same region), across a comparable range of altitudes. These flights followed a similar trend, showing elevated levels close to the ocean surface as opposed to levels at higher altitudes, however concentrations did not reach the same level of enhancement as flight B1. The variability in HC(O)OH concentration observed over the ocean may give further insight into the source type and origin, however this will be discussed further in sections 4.2–4.5.

4.2. Seasonal variation and the impact of biogenic sources to the Arctic budget

As illustrated by Table 3, mean concentrations (one times the standard deviation) for winter and summer were calculated as 86 ($\pm$68) ppt and 104 ($\pm$65) ppt respectively. Based on modelled predictions (Stavrakou et al., 2011), concentrations over the European Arctic are expected to show similar concentrations to that of Greenland. The mean summer concentration obtained in this study however is a factor of ten lower than previously reported summer measurements at Summit, Greenland (Dibb et al., 1994). Land measurements at altitudes $\leq$1.5 km revealed a weak enhancement of 22 ppt when changing to the growing season, although this is within the standard deviation. Likewise, data collected over a marine environment at altitudes $\leq$1.5 km revealed a small

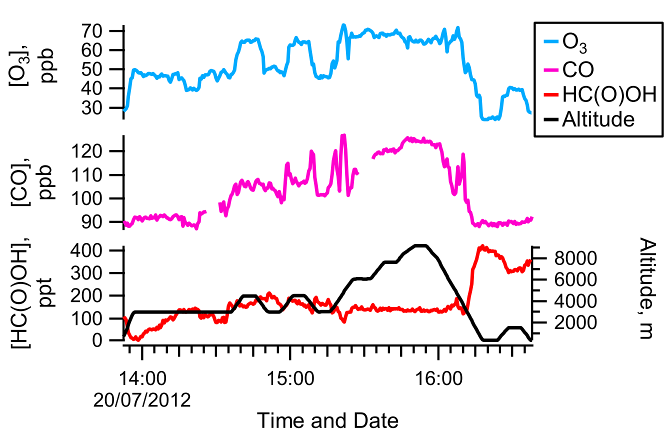

Fig. 11. Illustrating the concentration change in HC(O)OH during flight B1with respect to altitude and the trace gas species; O_3 and CO concentrations.

Table 3
Averaged mean HC(O)OH concentrations (ppt) collected during the March and July campaigns over the European Arctic.

	Winter		Summer	
Altitude range, km	$\leq$7 km data	$\leq$1.5 km data	$\leq$7 km data	$\leq$1.5 km data
Marine & continental data	86 $\pm$ 68	73 $\pm$ 63	104 $\pm$ 65	108 $\pm$ 65
Continental data	77 $\pm$ 65	49 $\pm$ 34	61 $\pm$ 33	71 $\pm$ 24
Marine data	103 $\pm$ 69	109 $\pm$ 78	131 $\pm$ 65	129 $\pm$ 71

enhancement of 20 ppt during the summer measurements, once more lying within the standard deviation range. Low altitude HC(O)OH levels were often independent of O_3 and CO concentrations which would indicate that local anthropogenic effects were of little significance. Biogenic emission from tree species (particularly the Norwegian Spruce), wetland and soils are likely to enhance HC(O)OH concentrations in the growing season; however results from this study would suggest these source types are not contributing significantly in the July period.

4.3. Marine vs continental contribution to the Arctic HC(O)OH budget

No significant elevations in HC(O)OH were observed over land, which included forest and wetland environments, during the summer campaign. Perhaps unexpectedly, mean concentrations at altitudes $\leq$1.5 km over land were found to be lower than the marine data in both the winter and summer seasons. Over land, concentrations at altitudes $\leq$1.5 km were on average 46% lower in the summer and 55% lower in the winter, in comparison with marine HC(O)OH concentrations. Furthermore, the highest observed HC(O)OH peak at altitudes $\leq$1.5 km across both campaigns was 420 ppt, collected in summer at 0.4 km altitude above the ocean surface. This is significantly greater than the highest concentration observed over land, peaking at 161 ppt during the winter. Concentrations over a marine environment also showed the greatest variability across both campaigns. These fluctuations over the ocean could possibly be attributed to marine micro biota emission. Phytoplankton blooms tend to be irregular, and can emit high concentrations of organic precursors that may be subsequently oxidised to yield HC(O)OH (Keene and Galloway, 1988). Phytoplankton levels are generally expected to be higher in the mid – to – high latitudes as opposed to levels near to the equator. Therefore, the observed seasonal pattern and variability over the ocean might be expected for the hypothesis of a marine biogenic source such as this. Alternatively, the summer enhancement over the ocean may also be attributed to oceanic release of CH_2I_2; its rapid photolysis releases CH_2I radicals that can react with O_2 to produce the criegee Intermediate, CH_2OO (Welz et al., 2012). Once formed, CH_2OO can either decompose in a unimolecular reaction or react with water to form HC(O)OH. There are currently very little documented measurements of CH_2I_2 emission, particularly over the open ocean. CH_2I_2 emission data are found to be highly variable with CH_2I_2 concentrations of 0.11 ppt up to 19.8 ppt at a location in Lilia (Latitude 48.6°N, Longitude 4.55°E, French Atlantic Coast) in Spring 2003. Other CH_2I_2 measurements include <0.08–1.02 ppt in the region of Spitzburgen (Schall and Heumann., 1993), 0.3–3.1 ppt at a coastal site in Dagebüll, Germany in Spring 2002 (Peters et al., 2005), as well as a concentration range as low as 0.02–0.36 ppt taken from a coastal site at Mace Head, Ireland (Carpenter et al., 1999). Based on these reported data a conservative concentration range between 0.5 and 5 ppt of CH_2I_2 was selected to estimate the HC(O)OH concentration produced from this source. An additional HC(O)OH estimate was made with respect to the maximum

Table 4
Estimated HC(O)OH concentrations (ppt) resulting from oceanic release of CH_2I_2 reacting to produce HC(O)OH, at latitude 70°N in the European Arctic for the 14th March 2012 and the 21st July 2012, based on modelled CH_2I_2 photolysis rates for 8 am and 12 pm respectively. Calculations were based on reported values for k_6 and k_5 of 1×10^{-16} cm^3 molecules^{-1} s^{-1} and 100 s^{-1} respectively (Percival et al., 2013). The [H_2O] was calculated based on an average atmospheric water vapour concentration of 5000 ppm converted to molecules cm^{-3} using standard pressure and average ground temperatures of 269 K and 282 K for March and July respectively.

Initial [CH_2I_2] ppt	[HC(O)OH]$_{(estimated)}$ at latitude 70°N for the 14th March 2012 ppt		[HC(O)OH]$_{(estimated)}$ at latitude 70°N for the 21st July 2012 ppt	
	8 am ($J = 1.2 \times 10^{-4}$ s^{-1})	12 noon ($J = 1.5 \times 10^{-4}$s^{-1})	8 am ($J = 11.4 \times 10^{-4}$s^{-1})	12 noon ($J = 18.6 \times 10^{-4}$ s^{-1})
0.5	0.4	0.5	4.0	6.5
1	0.9	1.1	8.0	13.0
2	1.7	2.2	16.0	26.0
3	2.6	3.2	24.0	39.0
4	3.4	4.3	32.0	52.0
5	4.3	5.4	39.9	65.0
20	17.1	21.5	160.0	260.1

recorded CH_2I_2 peak observed in Lilia. Although it is accepted that this CH_2I_2 concentration is not necessarily representative of the Arctic Circle, this estimate is thought to provide insight into the potential impact of such levels in the Arctic. Photolysis rates of CH_2I_2 were determined using the TUV model (Tie et al., 2003), modelled for latitude 70°N for the periods of March and July during the campaigns as shown in Table 4. The maximum level of HC(O)OH that can be produced is obtained by the production rate divided by the loss frequency. Here we recognise that dispersion would reduce the local level of HC(O)OH, but the maximum local level from the mechanism can be obtained by the use of steady state approximations for CH_2OO and CH_2I. Reaction R4a is assumed in this calculation to represent a 20% conversion rate with respect to reaction R4b, which is identified as the term "f" ($f = 0.2$) (Shallcross, personal communication). Based on previously calculated estimates, the rate constants for reactions R5 and R6 are $k_5 = 100$ s^{-1} (Percival et al., 2013) and $k_6 = 1 \times 10^{-16}$ cm^3 molecule^{-1} s^{-1} (Stone et al., 2014) respectively. Although, it is acknowledged that k_5 is not well constrained at present. k_7 (3.6×10^{-6} s^{-1}) represents the loss rate of HC(O)OH with regards to its atmospheric lifetime of 3.2 days.

$$CH_2I_2 + h\nu \rightarrow CH_2I + I \qquad \text{R3}$$

$$CH_2I + O_2 \rightarrow CH_2OO + I \qquad \text{R4a}$$

$$CH_2I + O_2 \rightarrow CH_2IOO \qquad \text{R4b}$$

$$CH_2OO \rightarrow \text{products} \qquad \text{R5}$$

$$CH_2OO + H_2O \rightarrow HC(O)OH + H_2O \qquad \text{R6}$$

$$f = \frac{k_{4a}}{k_{4a} + k_{4b}} = 0.2 \qquad \text{R7}$$

$$[HC(O)OH]_{max} = \frac{J[CH_2I_2]k_6[H_2O]f}{k_7(k_5 + k_6[H_2O])} \qquad \text{R8}$$

Calculated estimates of HC(O)OH production via CH_2I_2 photolysis would suggest that a concentration of 1–2 ppt (CH_2I_2) could account for the 20 ppt HC(O)OH enhancement observed across the campaigns from March to July 2012 at 70ºN latitude. In assuming an upper limit CH_2I_2 emission of 20 ppt, as observed in the European mid latitude (48.6ºN), an emission of this magnitude could result in an HC(O)OH production of 260.1 ppt, suggesting CH_2I_2 emission may represent a significant secondary production pathway for HC(O)OH. The variability observed in the CH_2I_2 emission data from previous studies is also comparable to the variability observed in HC(O)OH concentrations collected over the ocean during the MAMM campaign, thus providing further support for the hypothesis of a significant marine HC(O)OH source via CH_2I_2 photolysis. The limitation of satellites to measure accurately over the ocean emphasises the uncertainty surrounding marine sources on the HC(O)OH budget. The higher HC(O)OH concentrations over the ocean observed in this study would suggest marine sources dominate in comparison to land sources in the European Arctic. Therefore CH_2I_2 photolysis may represent an important production pathway for HC(O)OH, impacting the European Arctic budget.

4.4. Snow source investigation

Consistent snow cover was observed across all land areas studied throughout the winter campaign. Therefore land data collected in this study was used to investigate the contribution of a snow source to the European Arctic HC(O)OH budget. No HC(O)OH plumes were observed during the winter flights (other than those discussed) which would indicate the air masses were well mixed, and unaffected by strong emission events. The region measured is predominantly rural with only a few small towns located in the region, therefore based on the observed data HC(O)OH concentrations are unlikely to be influenced by local anthropogenic sources. Fig. 12 represents a vertical profile up to 1.5 km altitude of all the data collected in winter over land, and illustrates a marginal HC(O)OH increase of 17 ppt at the lowest altitude bin of 0.3–0.6 km in comparison to the 0.6–0.9 km altitude bin and thereafter. Albeit

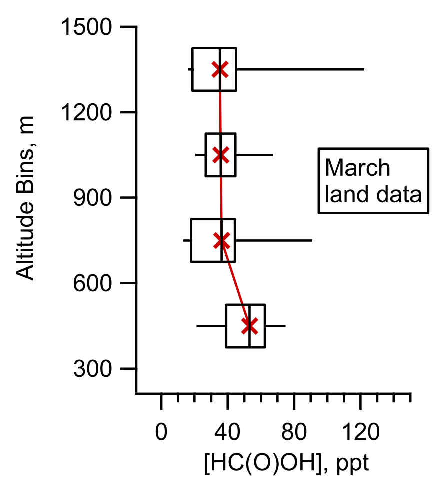

Fig. 12. Vertical profile of measurements during the MEVALI (March) campaign over land, arranged into 0.3 km altitude bins, where the box and whisker plots are divided into 10% and 90% percentiles, 25% and 75% percentiles represented by the box, the median represented by the central line within the box and the mean is represented by the x highlighted in red. (For interpretation of the references to colour in this figure legend, the reader is referred to the web version of this article.)

relatively small, this rise at low level would suggest a local emission influence. The mean HC(O)OH concentration over land at low level (0.3–1.5 km) during the winter campaign was found to be 49 (±34) ppt, as shown in Table 3. This is significantly lower than previously reported concentrations over the Greenland snowpack (Gao et al., 2012; Dibb et al., 1994, 1998). Furthermore the maximum winter concentration reported at altitudes ≤0.5 km over snow covered land was found to be 269 ppt. The maximum summer concentration reported over the ocean was found to be 468 ppt, a factor of 1.7 times higher than the winter maximum at the same altitude bin. This reaffirms the influence of seasonality to the local sources in the European Arctic and would indicate local winter emissions are low. These conclusions together with the expansive area covered in this study between latitudes 63–78°N and longitudes 11–29ºE in March would suggest that an HC(O)OH snow source in the European Arctic was not a significant contributor to the regional annual budget. Although it must be noted that aircraft data can be somewhat obscured by vertical mixing, surface exchange and transport, all of which complicate source identification and interpretation, and therefore constrained ground studies are required to confirm these findings.

4.5. Long range transport influence

Vertical profiles of the collective HC(O)OH data for each campaign are illustrated by Fig. 13A and B. These graphs show HC(O)OH enhancements at altitudes greater than 2 km across both campaigns, suggestive of possible long range source influence. The highest mean HC(O)OH concentration at altitudes greater than 2 km during the March and July campaigns were 132 ppt (within the 3–3.5 km altitude bin), and 176 ppt (within the 6–6.5 km altitude bin) respectively. These levels are higher than the reported satellite measurements in 2005 at 5.5 km for this latitude with mean concentrations of approximately 90 ppt and 50 ppt for March and July respectively (Gonzalez Abad et al., 2009). As shown in Table 3, the winter mean concentration for data collected across all altitudes was 28 ppt higher than the mean concentration across altitudes ≤1.5 km, indicative of an active high altitude source, likely from long range transport. Furthermore, the mean summer concentration collected across all altitudes was 2 ppt higher than the mean concentration collected at altitudes of ≤1.5 km. Typically HC(O)OH is expected to decrease with altitude due to its relatively short lifetime of 3.2 days in the free troposphere as well as increased mixing and dilution as it moves further from its source origin. These results however show a slight increase with altitude, suggesting high altitude sources are likely influencing both the winter and summer measurement period. As discussed for flights A2 and A5, four day HYSPLIT backward trajectories of observed elevations at altitudes greater than 2 km, remained at high altitudes and often travelled outside of the Arctic Circle. Therefore it is likely that long range sources from outside of the European Arctic may be responsible for these observed levels and are potentially important contributors to the European Arctic HC(O)OH budget, particularly during the winter. In summary, results from these campaigns over the European Arctic would suggest that local land sources do not significantly contribute to the regional HC(O)OH budget, and instead marine sources and the contributions from possible long range sources are likely to dominate.

4.6. HC(O)OH vertical profiles for this latitudinal bin (flight B3)

In this paper, two altitude profiles of HC(O)OH are presented within the European Arctic, off the coast of Svalbard on 21st July 2012 between the hours 14:05–14:58 utc, as illustrated by Fig. 14. To our knowledge, this work represents the first HC(O)OH real – time vertical profiles between the altitudes 0.35–6.6 km in the European Arctic; in the view to providing a more representative HC(O)OH profile for this latitudinal bin, and to provide new data contributions to improve global model studies and assist in satellite validation. Several hours prior to flight B3 on the 19th of July 2012, Svalbard had recorded 0.7 mm of precipitation occurring in the early hours of the morning, likely reducing HC(O)OH levels. HYSPLIT backward trajectories showed the air mass from each profile predominantly travelled from a clean-sector eastward direction, largely of marine origin. Analysis of vertical profiles and possible source contributions are included in order to assess any events which may bias this profile.

During the profile ascent, wind speed and direction remained relatively constant with an average speed of 7.7 (±3.0) m s^{-1} from a 269° (±17) direction. Low level stratocumulus clouds were observed sporadically during the profile, and dew point temperature and air temperature were used to identify periods within cloud. Average levels of O_3 and CO were 47.8 (±9.1) ppb and 98.7

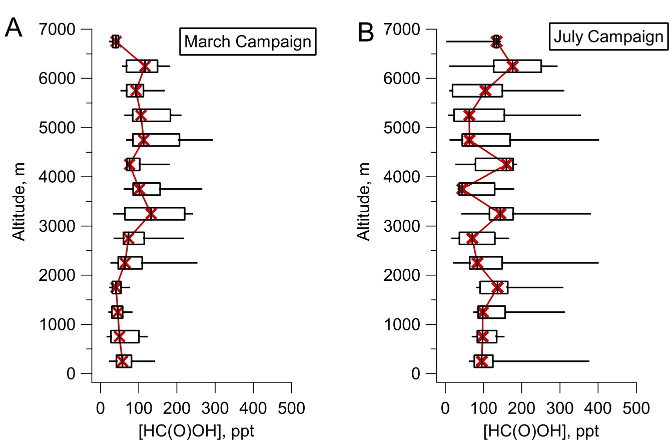

Fig. 13. A(left): HC(O)OH altitude profile for all the data collected during the March campaign, arranged into 0.5 km altitude bins over a 0.5–7 km range. B(right): illustrates the HC(O)OH altitude profile for all the data collected during the July campaign, arranged into 0.5 km altitude bins over a 0.5–7 km range. The box and whisker plots are divided into 10 and 90% percentiles, 25% and 75% percentiles represented by the box, the median represented by the central line within the box and the mean is represented by the x highlighted in red. (For interpretation of the references to colour in this figure legend, the reader is referred to the web version of this article.)

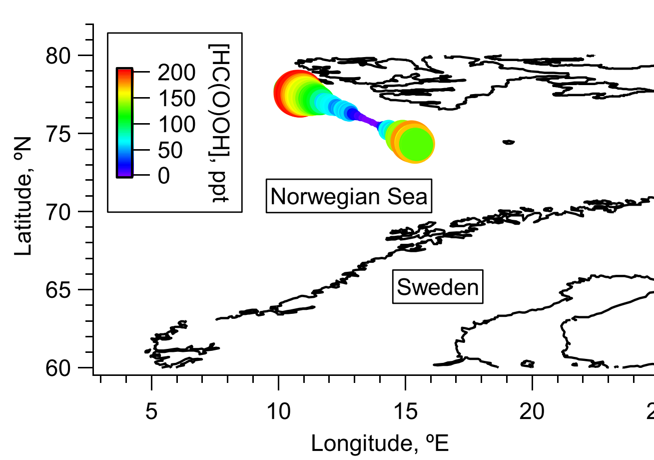

Fig. 14. Flight track of the altitude profile during flight B3 (19th July 2012), colour coded to HC(O)OH concentration in ppt, and sized to altitude ranging between 0.3(small) – 6.5(large) km. (For interpretation of the references to colour in this figure legend, the reader is referred to the web version of this article.)

(±3.6) ppb respectively as shown by Fig. 15A. An HC(O)OH enhancement of 22 ppt was observed between the altitudes 5–5.5 km, correlating with a 13 ppb rise in O_3 at the same point in time. This would suggest secondary production via ozonolysis may have contributed. HYSPLIT backward trajectories of this elevation identify the plume was likely four days old, originating from Russia in the region of the industrial city; Kanadalaksha. In assuming this HC(O)OH elevation was sourced from propene ozonolysis, a second order rate equation can be used, as shown by R9, to calculate the initial propene concentration required for the observed data, based on documented rate constants for propene ozonolysis (Neeb and Moortgat, 1999).

2nd Order Rate Equation.

$$[\text{Alkene}]_{\text{initial}} = \frac{k_7[\text{HC(O)OH}]_{\text{observed}}}{g\, k_{O_3}[O_3]} \quad g = \left(\frac{k_6[H_2O]}{(k_5 + k_6[H_2O])}\right) \tag{R9}$$

This calculation resulted in an initial propene concentration of 173 ppt, within expected propene emissions from urban environments, thereby representing a likely source contribution (Cullen, 1993; Collins et al., 1997; Johns et al., 1997). The lower concentrations observed at higher altitudes are likely due to increased mixing and dilution as the air parcel moves further afield from its source. With the exception of this secondary production source influence at altitudes 5–5.5 km, O_3 and CO levels were at background levels and relatively stable, indicative of a well-mixed air mass likely from a non-urban environment. HC(O)OH levels predominantly decreased with altitude, anti-correlating with CO and O_3 at altitudes greater than 1 km, suggesting the HC(O)OH levels were not significantly influenced by secondary production via ozonolysis or indeed by anthropogenic activity. The HC(O)OH maximum concentration was observed at 1 km altitude, with an enhancement of 67 ppt from the lowest altitude measurement. An HYSPLIT backward trajectory from 1 km altitude at time 16:00 utc, indicated this peak was a day aged plume from an eastward origin over the ocean. This peak corresponds with low O_3, suggesting the peak is likely from a direct emission source. The peak and subsequent decrease at higher altitudes would suggest this observation resulted from a weak, locally based, direct source, likely of biogenic origin. Therefore a simple first order calculation can be applied to estimate the source concentration, as shown in R10. Assuming a free troposphere lifetime of 3.2 days for HC(O)OH (Paulot et al., 2011), the direct source concentration was calculated to be 125 ppt, within recorded concentrations collected over the ocean (Baboukas et al., 2000).

$$[\text{HC(O)OH}]_{\text{initial}} = [\text{HC(O)OH}]_{\text{observed}} * e^{-kt} \tag{R10}$$

Although the ocean is considered an important source of HC(O)OH, the mechanism of this process remains highly uncertain and due to the hydrophilic nature of HC(O)OH, the ocean under certain conditions is also likely to act as a suitable medium for wet deposition. Therefore we hypothesise that the concentration drop observed below 0.8 km during ascent; and below 0.6 km during the descent is likely due to deposition to the ocean's surface. HC(O)OH release and abstraction within the ocean is complex and particularly difficult to evaluate due to the variations in ocean topography and the different types of organisms within the ocean, but results from this study would suggest the ocean may act as both a source and a sink.

The profile descent shows a comparable vertical profile of HC(O)OH with respect to the ascent profile, as shown by Fig. 15B. CO and O_3 concentrations were relative stable at background levels with average concentrations of 100.8 (±3.1) ppb and 43.4 (±5.8) ppb respectively. This once more would suggest a well-mixed air mass likely from a non-urban environment. HC(O)OH levels predominantly decreased with altitude, anti-correlating with CO and O_3 at altitudes greater than 1 km, suggesting the HC(O)OH levels were not significantly influenced by secondary production via ozonolysis or indeed by anthropogenic activity. These profiles may therefore provide an insight into a typical HC(O)OH profile across an altitude range of 0.3–6.6 km. Other than the elevations discussed, these measurements are free from strong emission source plumes and are therefore likely to represent a typical, well mixed vertical profile of HC(O)OH to help reduce the uncertainty of HC(O)OH trends with the European Arctic.

Further to this, an interesting phenomenon that presents itself from this profile study is the influence of cloud on the observed HC(O)OH concentrations. Previous studies have suggested clouds can act as a source of HC(O)OH via the reaction of formaldehyde and the hydroxyl radical in cloud drops (Chamedies and Davis, 1983). Conditions were stable, and no precipitation had occurred during measurement, signifying clouds were unlikely to act as a significant sink during the profiles. As shown during the ascent in Fig. 16A, below 5.5 km, the air and dew point temperature meet at two short periods between 2.6 – 2.7 km and 3.3–3.5 km representing predominantly cloud free conditions. This is confirmed by the on-flight camera positioned at the front of the aircraft. On the other hand, Fig. 16B (representing the profile descent) shows the reverse trend where air temperature and dew point temperature match throughout, confirming the heavy cloud conditions experienced above 1 km altitude; however HC(O)OH concentrations remained relatively unchanged. It must be noted however, that this cloud source mechanism is considered to be strongly pH dependent, therefore information on pH acidity would be required to fully assess this mechanism which was not obtainable in this study. Nevertheless, this study would suggest HC(O)OH concentration is independent of cloud under these conditions.

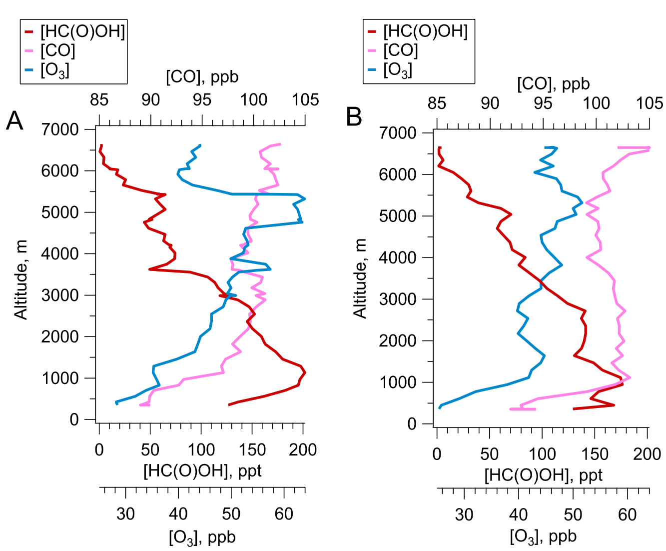

Fig. 15. A(left): illustrates the profile ascent in relation to HC(O)OH concentration in ppt, plotted alongside O_3 and CO in ppb during flight B3. B(right): illustrates the profile descent in relation to HC(O)OH concentration in ppt, plotted alongside O_3 and CO in ppb during flight B3.

5. Conclusions

These campaigns represent, to our knowledge, the first airborne measurements of HC(O)OH over the European Arctic, investigating seasonal differences over continental and marine environments.

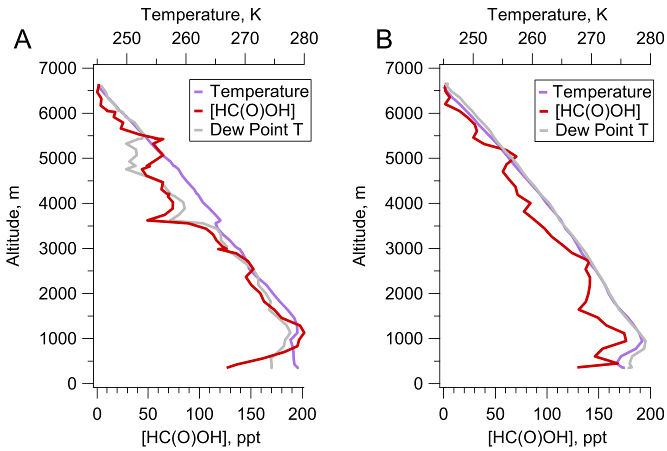

Fig. 16. A(left): illustrates the profile ascent in relation to HC(O)OH concentration in ppt, plotted alongside dew point temperature and air temperature in K during flight B3. B(right): illustrates the profile descent in relation to HC(O)OH concentration in ppt, plotted alongside dew point temperature and air temperature in K during flight B3.

The elevated HC(O)OH concentrations at high altitudes during both the winter and summer campaigns would suggest long range transport may play a significant role, particularly from northern Europe and Iceland. At altitudes ≤1.5 km, enhancements over land during the summer are likely due to expansive forests and possible wetland contributions, although their influence to the HC(O)OH budget in the European Arctic appears to be relatively low. The investigation into a possible snow source of HC(O)OH revealed no significant contribution to the local HC(O)OH budget. The maximum concentration observed over snow covered land during this study was 169 ppt; considerably lower than previously reported concentrations over the Greenland snowpack and the North American Arctic. Results instead would suggest marine sources dominate over local continental sources, with a maximum observed concentration during the summer of 420 ppt at 0.4 km above the ocean. The limitations of satellites to measure HC(O)OH accurately over the ocean highlights the necessity for in-situ, aircraft measurements over marine environments to ultimately assess the contribution of ocean sources to the HC(O)OH budget. Phytoplankton remains a potentially important marine source of HC(O)OH, particularly in the high latitudes where levels of phytoplankton are considered to be more enriched. Furthermore, this study highlights the potential impact of CH_2I_2 as a marine source. The role of CH_2I_2 in the European Arctic HC(O)OH budget remains uncertain however calculated estimates provided in this work would suggest it may represent an important marine source, influencing the Arctic HC(O)OH budget, although further datasets of HC(O)OH and CH_2I_2 emission are required to confirm these findings.

Acknowledgements

The authors would like to acknowledge Alan Knights for analysing the HC(O)OH calibration gas mixture using GC-FID analysis. We would also like to thank the FAAM staff for providing core aircraft data and their assistance in fitting the CIMS on-board the aircraft. Thanks also to the Met. Office, and NERC for their involvement in coordinating and funding the MEVALI and MAMM projects.

References

Andreae, M.O., Talbot, R.W., Andreae, T.W., Harriss, R.C., 1988. Formic and acetic acid over the central amazon region, Brazil 1. Dry season. J. Geophys. Res. 93, 1616–1624.

Baboukas, E.D., Kanakidou, M., Mihalopoulos, N., 2000. Carboxylic acids in gas and particulate phase above the Atlantic ocean. J. Geophys. Res. 105, 14459–14471.

Bannan, T.J., Bacak, A., Muller, J.B.A., Murray, A.M., Jones, B.T., Le Breton, M., Leather, K.E., Ghalaieny, M., Xiao, P., Shallcross, D.E., Percival, C.J., 2013. Importance of direct anthropogenic emissions of HC(O)OH measured by a chemical ionisation mass spectrometer (CIMS) during the Winter ClearfLo campaign in London, January 2012. Atmos. Environ. 83, 301–310.

Carpenter, L.J., Sturges, W.T., Penkett, S.A., Liss, P.S., Alicke, B., Hebestreit, K., Platt, U., 1999. Short lived alkyl iodides and bromides at mace head: links to macroalgal emission and halogen oxide formation. J. Geophys. Res. 104, 1679–1689.

Chamedies, W.L., Davis, D.D., 1983. Aqueous-phase source of HC(O)OH in clouds. Nature 304, 427–429.

Chebbi, A., Carlier, P., 1996. Carboxylic acids in the troposphere, occurrence, sources and sinks: a review. Atmos. Environ. 30 (24), 4233–4249.

Collins, W.J., Stevenson, D.S., Johnson, C.E., Derwent, R.G., 1997. Tropospheric ozone in a global scale three dimensional lagrangian model and its response to NO_x emissions controls. J. Atmos. Chem. 26, 223–274.

Cullen, M.J.P., 1993. The unified forecast/climate model. Meteorol. Mag. 122, 81–94.

Dibb, J.E., Talbot, R.W., Bergin, M.H., 1994. Soluble acidic species in air and snow at Summit, Greenland. Geophys. Res. Lett. 21, 1627–1630.

Dibb, J.E., Talbot, R.W., Munger, J.W., Jacob, D.J., Fan, S.-M., 1998. Air-snow exchange of HNO_3 and NO_y at Summit, Greenland. J. Geophys. Res. 103, 3475–3486.

Dibb, J.E., Arsenault, M., 2002. Shouldn't snowpacks be sources of monocarboxylic acids? Atmos. Environ. 39, 2513–2522.

Gao, S.S., Sjostedt, S.J., Sharma, S., Hall, S.R., Ullmann, K., Abbatt, J.P.D., 2012. PTR-MS observations of photo-enhanced VOC release from Arctic and midlatitude snow. J. Geophys. Res. 117, D00R17.

George, M., Clerbaux, C., Hurtmans, D., Turquety, S., Coheur, P.-F., Pommier, M., Hadji-Lazaro, J., Edwards, D.P., Worden, H., Luo, M., Rinsland, C., McMillan, W., 2009. Carbon monoxide distributions from IASI/METOP mission: evaluation with other space-borne remote sensors. Atmos. Chem. Phys. 9, 8317–8330.

Gonzalez Abad, G., Bernath, P.F., Boone, C.D., McLeod, S.D., Manney, G.L., Toon, G.C., 2009. Global distribution of upper tropospheric HC(O)OH from the ACE-FTS. Atmos. Chem. Phys. 9, 8039–8047.

Graedel, T.E., Weschler, C.J., 1981. Chemistry within aqueous atmospheric aerosols and raindrops. Rev. Geophys. Space Phys. 19, 505–539.

Grutter, M., Glatthor, N., Stiller, G.P., Fischer, H., Grabowski, U., Hopfner, M., Kellmann, S., Linden, A., von Clarmann, T., 2010. Global distribution and variability of HC(O)OH as observed by MIPAS-ENVISAT. J. Geophys. Res. 115, D10303. http://dx.doi.org/10.1029/2009JD012980.

Jacob, D.J., Wofsy, S.C., 1988. Photochemistry of biogenic emissions over the Amazon forest. J. Geophys. Res. 93, 1477–1486. http://dx.doi.org/10.1029/JD093iD02p01477.

Johns, T.C., Carnell, R.E., Crossley, J.F., Gregory, J.M., Mitchell, J.F.B., Senior, C.A., Tett, S.F.B., Wood, R.A., 1997. The second hadley centre coupled ocean-atmosphere GCM: model description, spinup and validation. Clim. Dyn. 13, 103–134.

Kawamura, K., Ng, L.-L., Kapian, I.R., 1985. Determination of organic acids (C1-C10) in the atmosphere, motor exhausts, and engine oil. Environ. Sci. Technol. 19, 1082–1086.

Keene, W.C., Galloway, J.N., 1988. The biogeochemical cycling of formic and acetic acids through the troposphere: an overview of current understanding. Tellus 40B, 322–334.

Kesselmeier, J., Bode, K., Gerlach, C., Jork, E.-M., 1998. Exchange of atmospheric formic and acetic acids with trees and crop plants under controlled chamber and purified air conditions. Atmos. Environ. 32, 1765–1775.

Leather, K.E., McGillen, M.R., Cooke, M.C., Utembe, S.R., Archibald, A.T., Jenkin, M.E., Derwent, R.G., Shallcross, D.E., Percival, C.J., 2011. Acid-yield measurements of the gas-phase ozonolysis of ethene as a function of humidity using chemical ionisation mass spectrometry (CIMS). Atmos. Chem. Phys. Discuss. 11, 25173–25204. http://dx.doi.org/10.5194/acpd-11-25173-2011.

Le Breton, M., McGillen, M.R., Muller, J.B.A., Bacak, A., Shallcross, D.E., Xiao, P., Huey, L.G., Tanner, D.J., Coe, H., Percival, C.J., 2011. Airborne observations of formic acid using a chemical ionisation mass spectrometer. Atmos. Meas. Tech. 4, 5807–5835.

Le Breton, M., Bacak, A., Muller, J.B.A., Xiao, P., Shallcross, B.M.A., Batt, R., Cooke, M.C., Shallcross, D.E., Bauguitte, S.J.-B., Percival, C.J., 2013a. Simultaneous airborne nitric acid and HC(O)OH measurements using a chemical ionization mass spectrometer around the UK: analysis of primary and secondary production pathways. Atmos. Environ. 83, 166–175.

Le Breton, M., Bacak, A., Muller, J.B.A., O'Shea, S.J., Xiao, P., Ashfold, M.N.R., Cooke, M.C., Batt, R., Shallcross, D.E., Oram, D.E., Forster, G., Bauguitte, S.J.-B., Palmer, P.I., Parrington, M., Lewis, A.C., Lee, J.D., Percival, C.J., 2013b. Airborne hydrogen cyanide measurements using a chemical ionisation mass spectrometer for the plume identification of biomass burning forest fires. Atmos. Chem. Phys. 13, 9217–9232. http://dx.doi.org/10.5194/acp-13-9217-2013.

Legrand, M., Preunkert, S., Jourdain, B., Aumont, B., 2004. Year-round records of gas and particulate formic and acetic acids in the boundary layer at Dumont d-Urville, coastal Antarctica. J. Geophys. Res. 109 http://dx.doi.org/10.1029/2003JD003786.

Neeb, P., Moortgat, G.K., 1999. Formation of OH radicals in the gas-phase reaction of propene, isobutene and isoprene with O_3: Yields and mechanistic implications. J. Phys. Chem. 103, 9003–9012.

Nowak, J.B., Neuman, J.A., Kozai, K., Huey, L.G., Tanner, D.J., Holloway, J.S., Ryerson, T.B., Frost, G.J., McKeen, S.A., Fehsenfeld, F.C., 2007. A chemical

ionization mass spectrometry technique for airborne measurements of ammonia. J. Geophys. Res. Atmos. 112, D10S02. http://dx.doi.org/10.1029/2006JD00758.
Paulot, F., Wunch, D., Crounse, J.D., Toon, J.C., Millet, B.D., DeCarlo, P.F., Vigouroux, C., Deutscher, N.M., Abad, G.G., Notholt, J., Warneke, T., Hannigan, J.W., Warneke, C., de Gouw, J.A., Dunlea, E.J., De Maziere, M., Griffith, D.W.T., Bernath, P., Jimenez, J.L., Wennberg, P.O., 2011. Importance of secondary sources in the atmospheric budgets of formic and acetic acids. Atmos. Chem. Phys. 11, 1989–2013.
Percival, C.J., Welz, O., Eskola, A.J., Savee, J.D., Osborn, D.L., Topping, D.O., Lowe, D., Utembe, S.R., Bacak, A., McFiggans, G., Cooke, M.C., Xiao, P., Archibald, A.T., Jenkin, M.E., Derwent, R.G., Riipinen, I., Mok, D.W.K., Lee, E.P.F., Dyke, J.M., Taatjes, C.A., Shallcross, D.E., 2013. Regional and global impacts of criegee intermediates on atmospheric sulphuric acid concentrations and first steps of aerosol formation. Faraday Discuss. 165, 45–73. http://dx.doi.org/10.1039/c3fd00048f.
Peters, C., Pechtl, S., Stutz, J., Hebestreit, K., Hönninger, G., Heumann, K.G., Schwarz, A., Winterlik, J., Platt, U., 2005. Reactive and organic halogen species in three different European coastal environments. Atmos. Chem. Phys. 5, 3357–3375. http://dx.doi.org/10.5194/acp-5-3357-2005.
Razavi, A., Karagulian, F., Clarisse, L., Hurtmans, D., Coheur, P.F., Clerbaux, C., Muller, J.F., Stavrakou, T., 2011. Global distributions of methanol and HC(O)OH retrieved for the first time from the IASI/MetOp thermal infrared sounder. Atmos. Chem. Phys. 11, 857–872.
Sanhueza, E., Andreae, M.O., 1991. Emission of formic and acetic acids from tropical savannah soils. Geophys. Res. Lett. 18, 1707–1710. http://dx.doi.org/10.1029/91GL01565.
Schall, C., Heumann, K.G., 1993. GC determination of volatile organoiodine and organobromine compounds in Arctic seawater and air samples. J. Anal. Chem. 346, 717–722. http://dx.doi.org/10.1007/BF00321279.
Shallcross D. E., verbal communication.
Slusher, D.L., Huey, L.G., Tanner, D.J., Flocke, F.M., Roberts, J.M., 2004. A thermal dissociation-chemical ionization mass spectrometry (td-cims) technique for the simultaneous measurement of peroxyacyl nitrates and dinitrogen pentoxide. J. Geophys. Res. 109 (13), D19315. http://dx.doi.org/10.1029/2004JD004670.
Stavrakou, T., Müller, J.-F., Peeters, J., Razavi, A., Clarisse, L., Clerbaux, C., Coheur, P.F., Hurtmans, D., De Mazière, M., Vigouroux, C., Deutscher, N.M., Griffith, D.W.T., Jones, N., Paton-Walsh, C.D., 2011. Satellite evidence for a large source of HC(O)OH from boreal and tropical forests. Nat. Geosci. 5, 26–30.
Stone, D., Blitz, M., Daubney, L., Howesa, N.U.M., Seakins, P., 2014. Kinetics of CH_2OO reactions with SO_2, NO_2, NO, H_2O and CH_3CHO as a function of pressure. Phys. Chem. Chem. Phys. 16, 1139–1149. http://dx.doi.org/10.1039/C3CP54391A.
Talbot, R.W., Beecher, K.M., Hariss, R.C., Cofer III, W.R., 1988. Atmospheric geochemistry of formic and acetic acids in mid-latitude temperate site. J. Geophys. Res. 93, 1638–1652.
Talbot, R.W., Andreae, M.O., Berresheim, H., Jacob, D.J., Beecher, K.M., 1990. Sources and sinks of formic, acetic, and pyruvic acids over central Amazonia 2. Wet season. J. Geophys. Res. 95, 16799–16811.
Talbot, R.W., Vijgen, A.S., Hariss, R.C., 1992. Soluble species in the Arctic summer troposphere: acidic gases, aerosols, and precipitation. J. Geophys. Res. 97, 16531–16543.
Tie, X.X., Madronich, S., Walters, S., Zhang, R.Y., Rasch, P., Collins, W., 2003. Effects of clouds on photolysis and oxidants in the troposphere. J. Geophys. Res. 108 (D20), 4642. http://dx.doi.org/10.1029/2003JD003659.
Welz, O., Savee, J.D., Osborn, D.L., Vasu, S.S., Percival, C.J., Shallcross, D.E., Taatjes, C.A., 2012. Direct kinetic measurements of criegee intermediate (CH_2OO) formed by reaction of CH_2I with O_2. Science 335, 204–207.
Yienger, J.J., Levy, H., 1995. Empirical model of global soil biogenic NO*x* emissions. J. Geophys. Res. 100, 11447–11464. http://dx.doi.org/10.1029/95JD00370.